The Bimodality of the 100 hPa South Asia High and its Relationship to the Climate Anomaly over East Asia in Summer

Qiong ZHANG, Guoxiong WU

State Key Laboratory of Atmospheric Sciences and Geophysical Fluid Dynamics, Institute of Atmospheric Physics, Chinese Academy of Sciences, Beijing, China

and

Yongfu QIAN

Department of Atmospheric Sciences, Nanjing University, Nanjing, China

(Manuscript received 26 December 2000, in revised form 13 May 2002)

Abstract

The NCEP/NCAR pentad mean reanalysis data from 1980 to 1994 are employed to examine the activities of the 100 hPa South Asia High (SAH) during the boreal summer. The results show that there exists bimodality in the longitude location of the SAH. According to the two preferred regions for the SAH, the SAH is classified into the Tibetan Mode (TM) and the Iranian Mode (IM), respectively. The studies on the maintenance mechanism, both from circulation structure and thermal structure, manifest that the SAH has the feature of warm preference. The diagnosis based on the thermodynamic equation further reveals that the TM is closely related to the diabatic heating of the Tibetan Plateau, whereas the IM is more associated with the adiabatic heating in the free atmosphere, as well as the diabatic heating near the surface.

The statistical composites, and case studies, corresponding to the two modes show that the SAH bimodality is strongly related to the climate anomalies over East Asia. In the case of TM, the southerly airflow over the subtropics and the northerly airflow over the middle-high latitude at 850 hPa are enhanced, forming a convergence zone along 30°N and resulting in increased rainfall extending from the south Japan, Korea Peninsula, and Yangtze-Yellow river valley of China to the Tibetan Plateau. In the case of IM, at 850 hPa the mid-latitude East Asia is dominated by a huge anomalous anticyclone, thus results in the decreased rainfall over the area.

1. Introduction

In summer in the upper troposphere, and lower stratosphere, there exists a large scale high pressure system (Tibetan High) over the Tibetan Plateau and its surrounding area, which is referred to the South Asia High (SAH) in this paper hereafter. Flohn (1960) suggested that the formation of the huge anticyclone is a result of the elevated heating of the Tibetan Plateau to the atmosphere. Based on the analyses of the International Geophysical Year (IGY) data, it has been recognized that the SAH is the strongest and the steadiest circulation system at the 100 hPa level besides the polar vortex (Mason and Anderson 1963). Tao and Zhu (1964) reported that the longitudinal

Corresponding author and present affiliation: Qiong Zhang, Center for Climatic Research, University of Wisconsin-Madison, 1225 W. Dayton St., Madison, WI 53706-1695, USA.
E-mail: joan@enso.meteor.wisc.edu

shifting of the SAH leads that of the 500 hPa Subtropical Anticyclone over Western Pacific (SAWP) for a few days, so that the activity of the SAH could be used as an index for the short-medium range weather forecasts in Asia. The longitudinal shifting of the SAH towards or apart from the Tibetan Plateau is then suggested as an east-west oscillation during the midsummer (commonly from July to August in the Northern Hemisphere) (Tao and Zhu 1964). Based on the daily 100 hPa synoptic charts published by the China Meteorological Observatory, Luo et al. (1982) further classified the SAH into three circulation patterns: the eastern pattern; western pattern; and belt-type pattern. The maintaining period for one pattern is about 10∼13 days, which is close to the 13∼15 days oscillation period of the stream function over the Tibetan Plateau revealed by Krishnamurti et al. (1973).

It is well known that the SAWP at 500 hPa level is a substantially important system influencing the summer rainfall variability over East Asia. Since there exist difficulties in forecasting the activity of SAWP (Liu and Wu 2000), the relationship between the east-west oscillation of the 100 hPa SAH, and the activities of SAWP, provides some new clues on the short-term prediction of the flood and drought occurring in this region in summer. Thus, the studies on the effects of the east-west oscillation of the SAH on summer precipitation have drawn intensive attentions. For example, during the Qinghai-Xizang Plateau Meteorology Experiment (QXPMEX) in 1979, many synoptic analyses were conducted based on the observation data, and most results have been applied to routine forecasts (Zhao et al. 1978; Zhu et al. 1980; Luo et al. 1982; Chen et al. 1983; Xu 1983; Yang et al. 1984).

Besides the synoptic analyses mentioned above, the mechanism responsible for the east-west oscillation of the SAH was also studied. The arguments fall into two basic categories concerning whether thermal effect, or dynamical forcing of the Tibetan Plateau is more important for the oscillation. The thermal forcing proponents emphasize the huge sensible heating of the Tibetan Plateau, which causes the adjustment of the subtropical circulation, together with the effects of the latent heating over the eastern China plain, resulting in the east-west oscillation (Qian et al. 1978; Liu et al. 1987). The dynamical forcing proponents think much of the interaction between the circulation systems (Institute of the Central Meteorological Bureau of China 1978), they suggested that the adjustments of the nearby circulation induced by the Plateau cause a kind of forcing oscillation that is different from the self-oscillation due to its thermal forcing. The case study shows that such a forcing oscillation may be related to the eccentric effect of the Northern Hemisphere polar vortex. Some of the possible mechanisms have also been suggested based on the dishpan experiments (Zhang et al. 1977), which show that an obstacle can independently produce a kind of oscillation without thermal effect. However, such an oscillation is confined to a small range, and the center of the SAH can hardly move out of the Tibetan Plateau. In contrast, a distinct large range of oscillation occurs, when the external circulation effect is included into the dishpan experiment.

Recently, we examined the climatic characteristics of the SAH by employing the 40-year NCEP/NCAR reanalysis. It is found that the SAH exhibits as bimodality in longitude location during the northern summer, one location is over the Tibetan Plateau, and another over the Iranian Plateau. Such bimodality is different from the east-west synoptic oscillation as suggested by Tao and Zhu (1964). The importance of the SAH bimodality also lies on its close relation with the large area occurrence of flood and drought (Zhang and Wu 2001). Therefore, it is necessary to study further the features of the bimodality, as well as the mechanism of the alternation from one mode to another.

In this work, we present the SAH bimodality by using NCEP/NCAR pentad mean reanalysis data. Some diagnostic methods described in section two are applied to study its thermal, and dynamical structure. Section three presents the description of the bimodality. The thermal and dynamical features of the SAH are addressed in section four. Section five presents the association of the bimodality with the climate anomaly in Asia. The possible connection between the SAH bimodality, and the climate anomaly over Asia, is described in section six via case study. Section seven lists the main summary of this study.

2. Data and methods

2.1 Data

The pentad mean data for this study comes from the NCEP/NCAR daily reanalysis set (Kalnay et al. 1996), covering the 15-yr period from 1980 to 1994. The reanalyses were obtained by assimilating past data into a frozen state-of-the-art analysis/forecast model system. The database was enhanced with many sources of observations that were not available in real time operations, and the products can be regarded as one of the most complete, physically consistent meteorological datasets. To establish the pentad mean reanalysis, the daily mean data are recomputed by arithmetical mean. For the purpose of convenience, six pentads are uniformly distributed in each month, a pentad value is usually obtained from the corresponding 5-day mean, for those 31-day months, the sixth pentad values are obtained from the corresponding 6-day mean, and for a 28-day or 29-day February, the sixth pentad value is obtained from 3- or 4-day mean.

Considering the planetary scale of the SAH during summer, the domain of 40°–140°E, 20°S–60°N is chosen to capture the main activities of the SAH. The geopotential height, wind and air temperature data at the standard pressure levels (1000, 850, 700, 500, 400, 300, 200 and 100 hPa) are analyzed objectively on a $2.5^\circ \times 2.5^\circ$ lat-lon resolution. Besides, the NCEP surface temperature are analyzed on a 192×94 Gaussian grid.

The pentad mean rainfall data on a $2.5^\circ \times 2.5^\circ$ lat-lon grid are obtained from the Climate Prediction Center Merged Analysis of Precipitation (CMAP) dataset (Xie and Arkin 1997). We used the version derived by merging rain gauge observation with rainfall estimates inferred from various satellite observations, but without numerical model outputs. Over land the data is mainly based on information from rain gauge observations, while over the ocean they primarily use satellite estimates made with several different algorithms based on outgoing longwave radiation, and scattering and emission of microwave radiation.

The anomalies throughout this study are referred to the departures from their corresponding 15-yr means.

2.2 Diagnostic methods

The thermal structure of the bimodality is examined based on the thermodynamic equation

$$\frac{\partial T}{\partial t} = -\vec{V} \cdot \nabla T - \left(\frac{P}{P_0}\right)^{\kappa} \omega \frac{\partial \theta}{\partial p} + \frac{Q_1}{C_P}, \tag{1}$$

where T is temperature, θ potential temperature, $\vec{V}$ horizontal wind, ω vertical p-velocity, $\kappa = R/C_P$, Q_1 diabatic heating, C_P the specific heat at constant pressure of dry air, $P_0 =$ 1000 hPa.

The velocity ω in (1) has been obtained kinematically by integrating the mass continuity equation (Haiyan H. et al. 1987)

$$D + \frac{\partial \omega}{\partial p} = \frac{1}{a \cos\phi}\left[\frac{\partial u}{\partial \lambda} + \frac{\partial}{\partial \phi}(v \cos\phi)\right] + \frac{\partial \omega}{\partial p} = 0, \tag{2}$$

with the surface boundary condition

$$\omega = \omega_S = -g\rho_S\left(\frac{u_S}{a\cos\phi}\frac{\partial h}{\partial \lambda} + \frac{v_S}{a}\frac{\partial h}{\partial \phi}\right) \quad \text{at } p = p_S. \tag{3}$$

In (2) and (3) u and v are the zonal and meridional components of horizontal wind $\vec{V}$, respectively, D horizontal divergence, a mean earth radius, ϕ latitude, λ longitude, p pressure, g acceleration of gravity, ρ density, and h terrain height. The suffix S denotes the surface value.

Assuming that the motion is approximately adiabatic in the layer between 100 and 200 hPa, we impose the additional condition near the tropopause

$$\omega = \omega_T = -\left(\frac{\partial \theta}{\partial t} + v \cdot \nabla\theta\right) \Big/ \left(\frac{\partial \theta}{\partial p}\right) \quad \text{at } p = p_T = 150 \text{ hPa}. \tag{4}$$

The original estimates of the horizontal divergence D_0 are corrected by adding

$$D' = \frac{\omega_T - \omega_S - \int_{p_T}^{p_S} D_0\, dp}{p_S - p_T}. \tag{5}$$

Then $D = D_0 + D'$ is used to obtain ω from (2).

3. Description of the bimodality

As shown in Fig. 1, in the multi-year mean 100 hPa geopotential height field, the midsum-

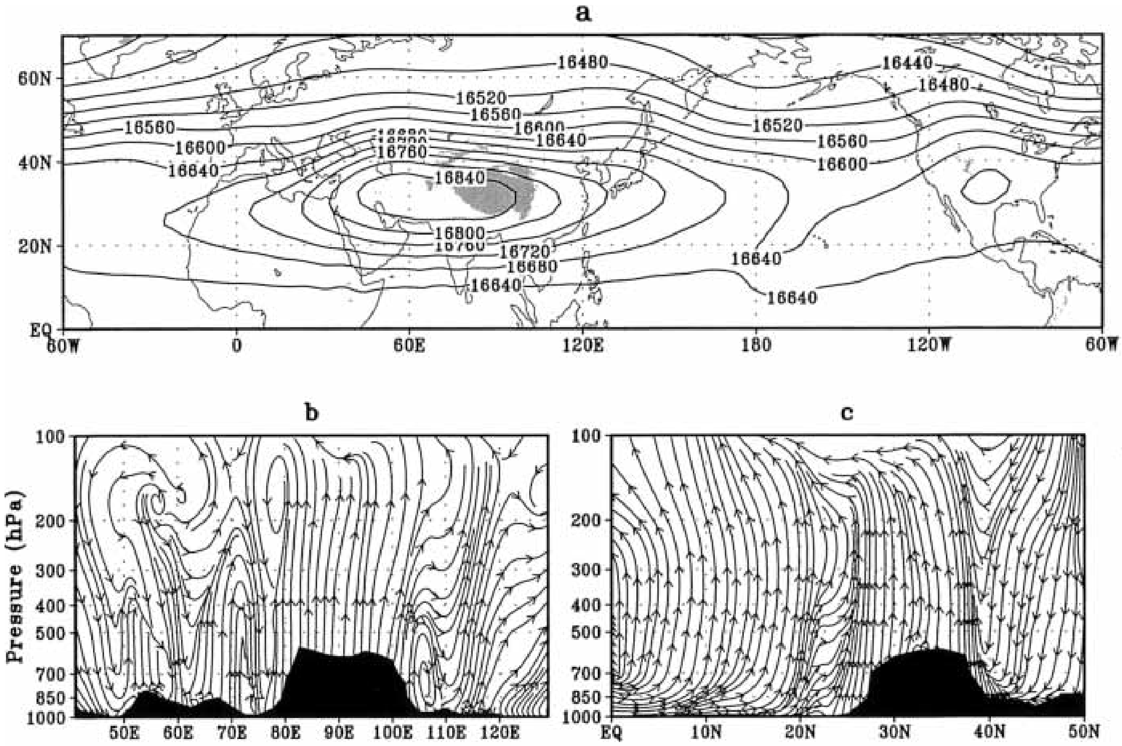

Fig. 1. (a) July–August mean 100 hPa geopotential height from the NCEP/NCAR pentad mean reanalysis for 1980–1994, unit: gpm. The topography greater than 3000 m are shaded. (b) The pressure-longitude section for the mean vertical circulation along 30°N. (c) The pressure-latitude section along 90°E. ω is amplified 150 times when plotting.

mer mean SAH which is centered over the Tibetan Plateau, and its neighborhood exhibits as a huge system covering most part of the subtropics in the Northern Hemisphere. Another high system lies over the Rocky Mountains with a much smaller scale. Such a distribution may imply that in summer the high system in the upper level is related to the large scale topography, and their thermal features may be deduced from such a morphological character.

Figure 1b and Fig. 1c respectively, show the zonal section of the mean vertical circulation along 30°N and meridional section along 90°E. The ascending motions related to the thermal effect of the highlands are observed in the area of the SAH. The strong ascending motion over the central Tibetan Plateau is up to 100 hPa (Fig. 1b). Due to the appearance of the topographic trapped wave, the ascending motions on the two sides of the Tibetan Plateau, are weakened to some extent. It is found that the ascending motion over the Iranian Plateau is limited only in the lower troposphere, and the descending motions are in dominant in the upper troposphere. In the meridional section (Fig. 1c), it is observed that a strong summer monsoon circulation expands over a large area extending from the Tibetan Plateau to the equator, again illustrating the considerable thermal effects of the Tibetan Plateau in summer. The above mean vertical circulations suggest that the maintenance of the SAH over the Tibetan Plateau, and its neighborhood, is mainly related to the thermal effects of the huge highland during summer.

Generally, the location of the SAH is described by its ridge line, and the center. At 100 hPa easterlies prevail in low latitudes, and westerlies prevail in mid-latitudes. The ridge line of the SAH is then defined as the interface between the easterlies and westerlies, and its center is found at a grid point where the geo-

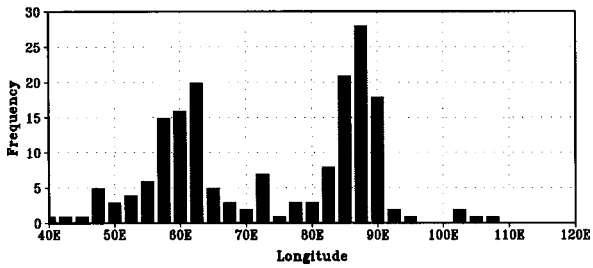

Fig. 2. The longitude-frequency distribution of the SAH major center during midsummer from the pentad mean data. For 15 summers there are totally 180 pentads involved in the statistics.

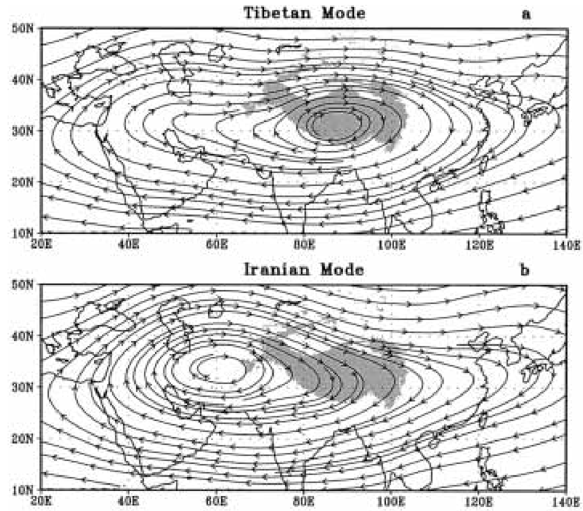

Fig. 3. The 100 hPa streamline composite corresponding to the TM (a) and the IM (b). 77 TM cases, and 62 IM cases are included in 1980–1994 July–August pentads.

potential height along the ridge line is the greatest. Thereby the location of the SAH center can be described by the longitude and latitude coordinates of the point.

When the activities of the SAH in summer are examined in detail by the individual pentad data, it is found that its longitude location exhibits as bimodality. Figure 2 shows the statistical frequency of the longitude location of the SAH in summer. The period considered for the statistics is July and August, which means there are 12 pentads in each midsummer, totally 180 pentads during 1980–1994. Quite similar to that of the monthly mean data (not shown), the SAH centers possess two preferable locations corresponding to the location of the Tibetan Plateau to the east and Iranian Plateau to the west, but scarcely appear near 70°–80°E, where the centered region of the climate mean SAH is located (Fig. 1a). According to its preferable location, the SAH can be classified into the Tibetan Mode (TM), and the Iranian Mode (IM), respectively. Those center longitudes lie between 82.5°–92.5°E, are defined as the TM, and the center longitudes that lie between 55°–65°E, are defined as the IM. Statistically, among the total 180 pentads there are 77 pentads for TM (42.8%), and 62 pentads for IM (34.4%).

The 100 hPa streamline composites for the two modes are shown in Fig. 3. Besides the remarkable planetary feature of the SAH, its location reflects the preference to the highlands. Moreover, it is observed that the IM lies more northward than the TM.

4. Thermal and dynamical structure of the bimodality

4.1 Vertical structure

To understand the thermal and dynamical features of the SAH bimodality, more composites for the two modes are presented in the following.

Figure 4 shows the pressure-longitude sections composed for the two modes along the ridge line latitude. Here we present the anomalies of the vertical circulation and the potential temperature to address the dynamical, and thermal structure of the TM and IM. It can be found that the TM corresponds to the anomalous strong ascending motion over the central Tibetan Plateau (Fig. 4a), which enhancing the original ascending motion over the region in Fig. 1b, and accompanied by the anomalous warm column (Fig. 4c). In the case of the IM, the anomalous ascending motions are observed over the Iranian Plateau (Fig. 4b), which weakens the original descending motion over the region in Fig. 1c, and also accompanied by the anomalous warm column. It is also found that contrasting to the tropospheric warm column, the SAH center at 100 hPa exhibits as a cold one (Fig. 4c, d). The above vertical struc-

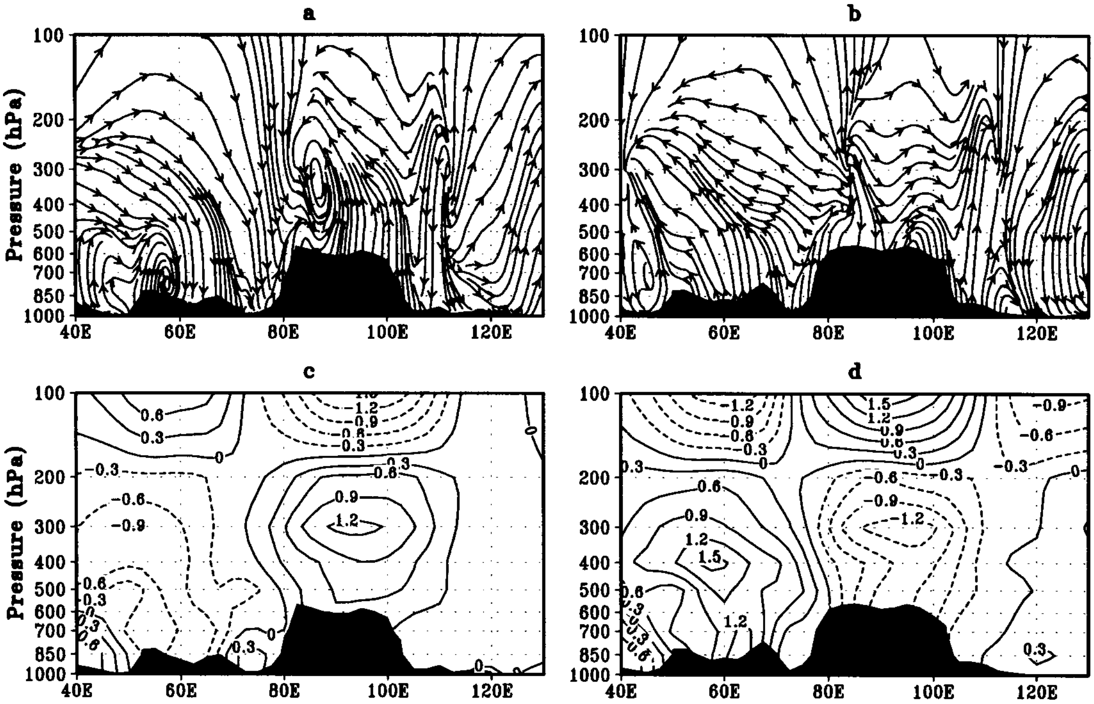

Fig. 4. The pressure-longitude cross sections composed for the TM (a and c, along 30°N) and the IM (b and d, along 32.5°N). a and b are vertical circulation anomalies, ω is amplified 150 times when plotting; c and d are potential temperature anomalies, unit is K. 77 TM cases, and 62 IM cases are included in 1980–1994 July–August pentads.

tures show that in both the TM and the IM case, the cold SAH center is corresponding to the anomalous ascending motions (Fig. 4a, b) and the anomalous warm column (Fig. 4c, d). In the other words, it indicates that the SAH has the feature of *warm preference*. It may suggest that the anomalous warm column is related to the SAH center via the anomalous ascending motion in the column. The anomalous ascending motions enhance the divergence at upper level, thus increase the negative vorticity at the region, and result in the maintenance of the anticyclone center over the region. Such a warm preference feature of the SAH is also demonstrated by the meridional section composites (not shown).

4.2 The thermodynamic equation diagnosis

To further examine the thermal characteristics of the SAH bimodality and the possible reason of the SAH's warm preference, the terms of the thermodynamic equation (1) are calculated. Figure 5 shows the pressure-longitude cross sections of the terms of Eq. (1) along the SAH ridge line latitude for the TM. It is found that the obvious warming occurs over the Tibetan Plateau up to 200 hPa. Figure 5d indicates that such a warming results from the diabatic heating over the Tibetan Plateau, while the strong cooling due to ascent over the Plateau shown in Fig. 5c compensates the diabatic heating to a large extent. The horizontal advection shown in Fig. 5b contributes only a small part to the warming. Therefore, it indicates that the contribution of the diabatic heating of the Tibetan Plateau, is much important to the maintenance of the TM.

Figure 6 shows the similar pressure-longitude cross sections for the IM. The warming center over the Iranian Plateau is located in the lower and middle troposphere (Fig. 6a), acting as a warm background for the IM, and also illustrating the warm preference of the SAH. Similar to the case of the TM, such a warming over the Iranian Plateau in the lower troposphere is mainly due to the *in situ* surface

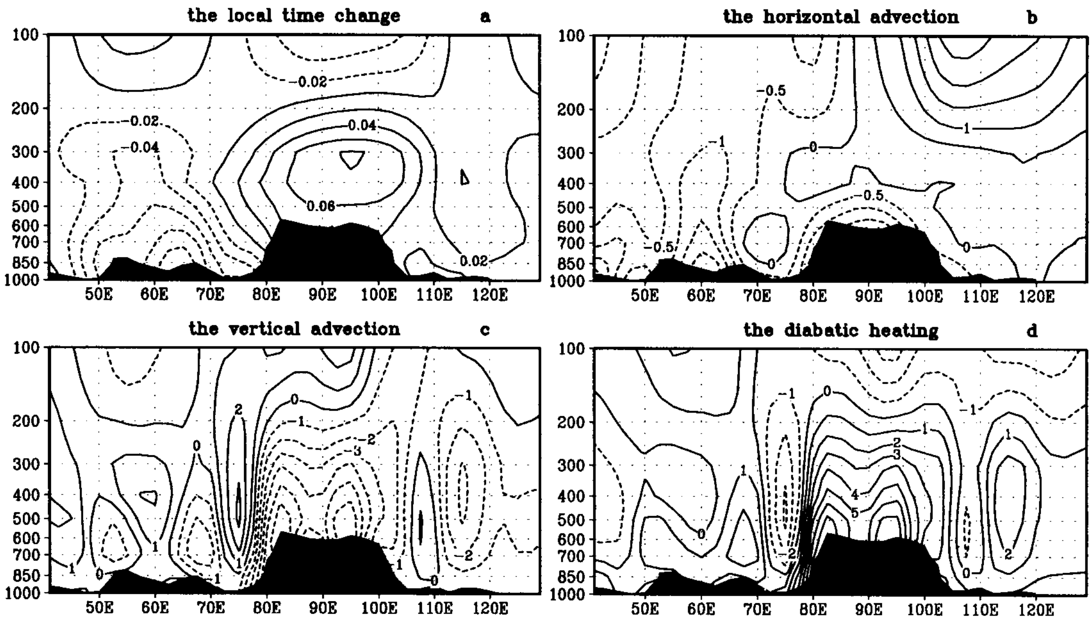

Fig. 5. The pressure-longitude cross sections composed for the terms in Eq. (1) along 30°N for the TM, unit is K/day. (a) Local time change, (b) horizontal advection, (c) vertical advection, and (d) diabatic heating. 77 TM cases, and 62 IM cases are included in 1980–1994 July–August pentads.

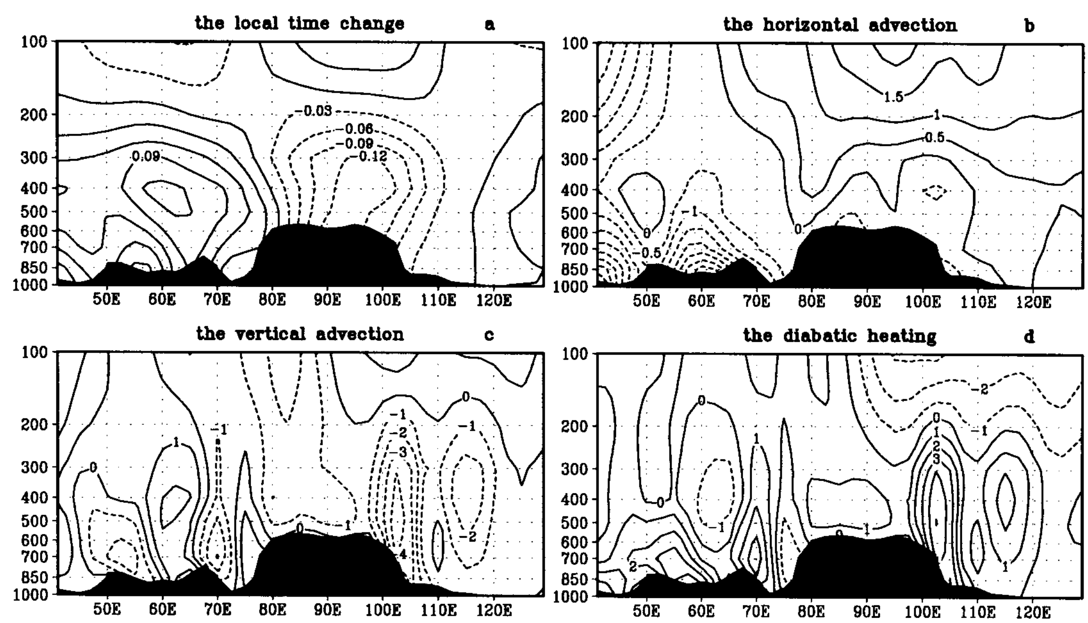

Fig. 6. Pressure-longitude cross sections composed for the terms in Eq. (1) along 32.5°N for the IM, unit is K/day. (a) Local time change, (b) horizontal advection, (c) vertical advection, and (d) diabatic heating. 77 TM cases, and 62 IM cases are included in 1980–1994 July–August pentads.

heating (Fig. 6d). However, unlike the case shown in Fig. 5d, the warming in the middle troposphere centered at 400 hPa over the Iranian Plateau (Fig. 6a) is mainly due to the *in situ* adiabatic heating (Fig. 6c), compensated by the horizontal advection (Fig. 6b) and diabatic cooling (Fig. 6d).

In summary, it is indicated that the center of the SAH tends to stay over the warm air column. For the TM, such a warming is mainly due to the diabatic heating over the Tibetan Plateau; whereas for the IM, besides the diabatic heating in the lower troposphere, the adiabatic heating associated with descent in the middle troposphere over the Iranian Plateau is more important. Therefore, the maintenance of the SAH over the certain region mostly depends on the thermal effect of the atmosphere over the region.

5. SAH bimodality and climate anomaly over Asia

To contrast the climate anomaly over Asia between the two SAH modes, we present composite maps of surface temperature, 850 hPa wind, and rainfall for 77 TM cases minus 62 IM cases. Because of the quite close case numbers of the two modes, in total 180 pentads, the anomalies associated with the TM, and the IM, tend to have opposite polarities. Thus, the composite TM-minus-IM will be simply referred to as dominant TM anomalies.

The differences of the surface temperature for the two modes show a distinct east-west contrast corresponding to the SAH center (Fig. 7a). It further confirms the warm preference of the SAH center as shown in Fig. 4c–d. The positive surface temperature anomalies are mostly associated with the enhanced near surface heat flux. Therefore, supporting the results shown in Fig. 5 and Fig. 6, it suggests that the diabatic heating over the Tibetan Plateau and the Iranian Plateau play an important role for the maintenance of the SAH over the two highlands.

As shown in Fig. 7b, a prominent cyclonic anomaly is found over middle latitude East Asia in 850 hPa wind difference between the TM and IM cases. The southerly airflows to the southeast of the cyclonic anomaly and the northerly airflows to the northwest of the cyclonic anomaly are significantly intensified. Such a wind anomaly brings about a convergence zone near 30°N along the lower reaches of the Yangtze River Valley, to south Japan. As a result, the large area differences of the rainfall for the two modes are found at the north and south side of 30°N (Fig. 7c). In the case of the TM, an enhanced rainfall belt extends from the northeast China, Korea Peninsula, and south Japan to the Yangtze-Yellow river valley, and the Tibetan Plateau. The composite rainfall difference attains a 95% significance level in most parts of these regions. To the south of 30°N, the rainfall increases in the case of the IM, however, only a few regions show the significant difference between the two modes. It suggests that the SAH bimodality is more related to rainfall anomalies over East Asia. It also noticed that significant differences are found near the Iranian Plateau at 850 hPa wind, whereas the rainfall over the area between the two modes has no much differences due to the rainless climate over this desert area.

6. Discussion

The statistical results show that the climate anomalies over East Asia are significantly related to the SAH bimodality. To illustrate how the 100 hPa SAH bimodality is connected to the rainfall anomaly over East Asia, two cases, July 1982 and July 1994 are chosen to have a comparison. Figure 8a shows that, in July 1982, the increased rainfall is distributed along a belt from south Japan, Korea Peninsula and Yangtze-Yellow river valley of China, to the Tibetan Plateau and India. Such a rainfall anomaly pattern corresponds with TM at 100 hPa, westward-extended SAWP at 500 hPa (Fig. 8b), and an anomalous anticyclone over subtropics at 850 hPa (Fig. 8c). Thus, the intensified southerly airflow in the subtropics, and northerly airflow in mid-high latitude, bring about the convergence zone near 30°N, as a result, the rainfall over this region is enhanced.

In contrast, in the case of July 1994, the rainfall over East Asia at mid-latitude such as Japan, Korea and Yangtze-Yellow river valley of China, is decreased (Fig. 8d). As shown in Fig. 8e, in this case, 100 hPa SAH presents as IM and 500 hPa SAWP weakens and withdraws eastward. At 850 hPa, a dominant anomalous anticyclone locates over the mid-

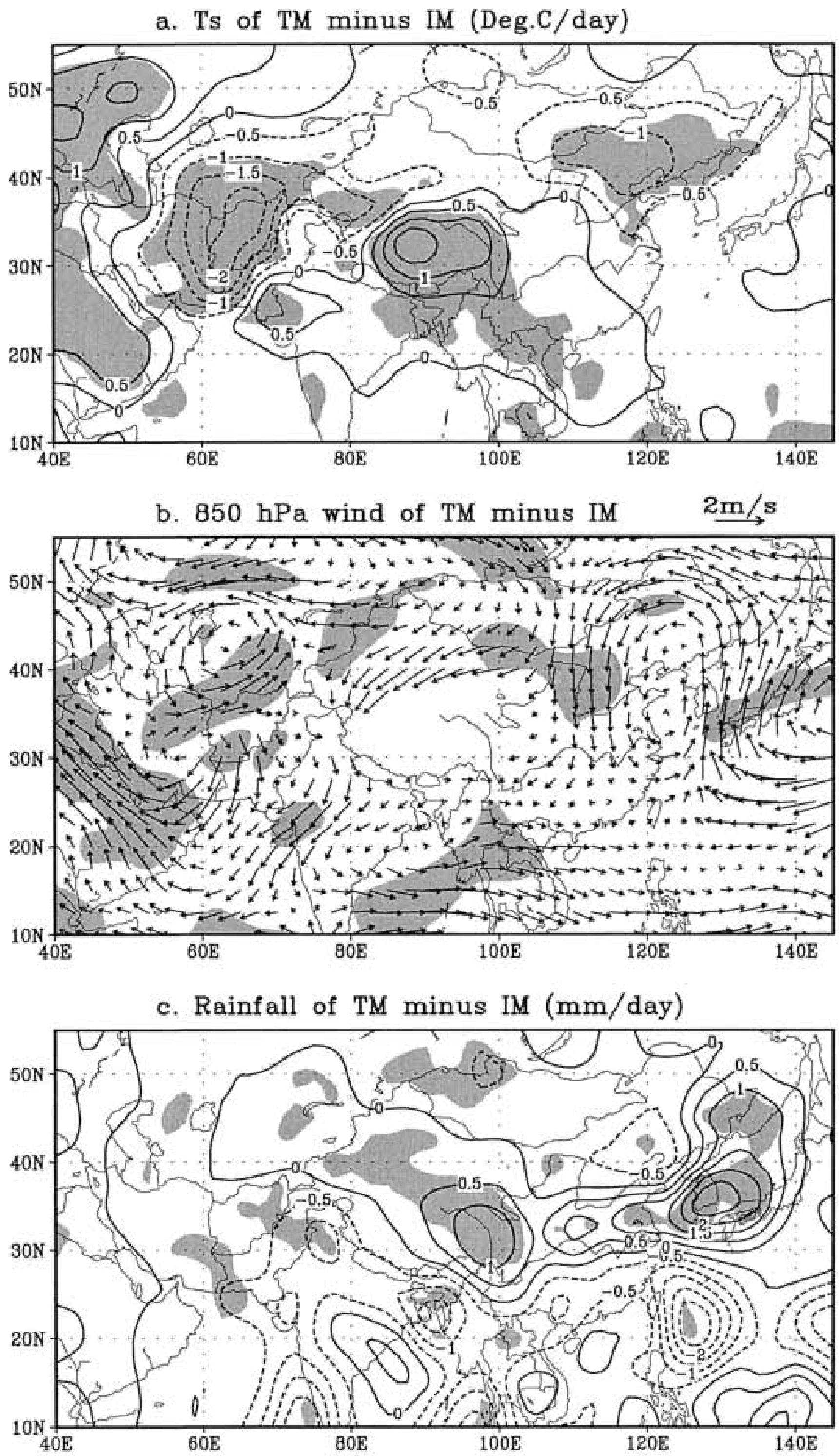

Fig. 7. Composite difference of (a) surface temperature, (b) 850 hPa wind and (c) rainfall between the TM and IM. Shading denote region of difference at 95% significance level. The wind vectors where the topography greater than 3000 m are set in default in (b). 77 TM cases, and 62 IM cases are included in 1980–1994 July–August pentads.

latitude East Asia, resulting in decreased rainfall over the area.

The results from the above case study are consistent with the statistical results in Fig. 7 over middle-high latitudes, especially over East Asia. However, some contradictions between the case study, and composite analysis are found over the tropics, both in rainfall and wind anomalies. It may suggest that the climate anomalies over East Asia are strongly related to the SAH bimodality, whereas the climate anomalies over the tropics may be more related to the tropical atmosphere anomaly.

In the above two case studies, the relationship between the 100 hPa SAH and the 500 hPa SAWP is similar to the viewpoint of Tao and Zhu (1964). That is, following the eastward (westward) shifting of the 100 hPa SAH, the 500 hPa SAWP behaves as westward extending (eastward withdrawing). Furthermore, it is noticed that the 500 hPa Iranian subtropical High also has the extending, and withdrawing behavior, following the shifting of the 100 hPa SAH (Fig. 8b and e). Such a relationship between the SAH bimodality and 500 hPa subtropical system is much important and helpful to short-term weather forecasting. However, the interaction process between the upper and middle-low level subtropical system remains a key issue and need to be further studied.

7. Summary

The pentad mean reanalysis data from NCEP/NCAR reanalysis are employed to examine the activities of the SAH during summer. The diagnoses show that there exists bimodality in the longitude location of the SAH. According to the two regions where the SAH preferring to stay, the SAH is classified into the Tibetan Mode, and the Iranian Mode, respectively. The studies on the maintenance mechanism both from circulation structure and thermal structure manifest that the SAH has the feature of warm preference. The diagnosis on the thermodynamic equation further reveals that the TM is closely related to the diabatic heating of the Tibetan Plateau, whereas the IM is more associated with the adiabatic heating in the free atmosphere as well as the diabatic heating near the *in situ* surface. The composite of the surface temperature for the two SAH modes suggests that the sensible heat over the Tibetan Plateau and Iranian Plateau may play an important role in the maintenance of the SAH over the two highlands.

The statistical analysis and the case study show that SAH bimodality is strongly related to the climate anomaly over East Asia. The TM corresponds with an increased rainfall belt extending from the south Japan, Korea and Yangtze-Yellow river valley to the Tibetan Plateau. In the case of IM, a decreased rainfall pattern is found over the above area.

The SAH bimodality presented in this study is substantially different to the previous east-west oscillation of the SAH on some aspects. First, the time scale is different: the bimodality distribution is examined based on climatological data, whereas the east-west oscillation is often referred as a synoptic process; second, the spatial scale is also different, the shifting scope of the bimodality extends much larger than that of the east-west oscillation, as shown in Fig. 2 and Fig. 3, the TM is located over the Tibetan Plateau centered at about 90°E, and the IM is near the Iranian Plateau centered at about 60°E. However, when the concept of east-west oscillation is first presented by Tao and Zhu (1964), it is suggested as the longitudinal shifting of the SAH towards and apart from the Tibetan Plateau. Their study emphasized the influence of the SAH on summer rainfall in China, and did not put much attention to far westward extension of the SAH to the Iranian Plateau. Third, the maintenance and variation mechanism of the bimodality and east-west oscillation differs considerably. Although the structure, and feature of the TM and IM are different, their preference to a certain region presents as a relatively steady status. The mechanism of the east-west oscillation as discussed in the introduction remains uncertain. In a parallel research, we further analyze the activity and feature of the Tibetan Mode in more details, and have found that all the TM cases can also be divided into two types: eastern TM and western TM types. The shifting between these two types and the spatial span of such shifting are more similar to the aforementioned west-east oscillation of the SAH. The conjecture about the east-west oscillation of the SAH on a climate time scale will be published in a separate paper.

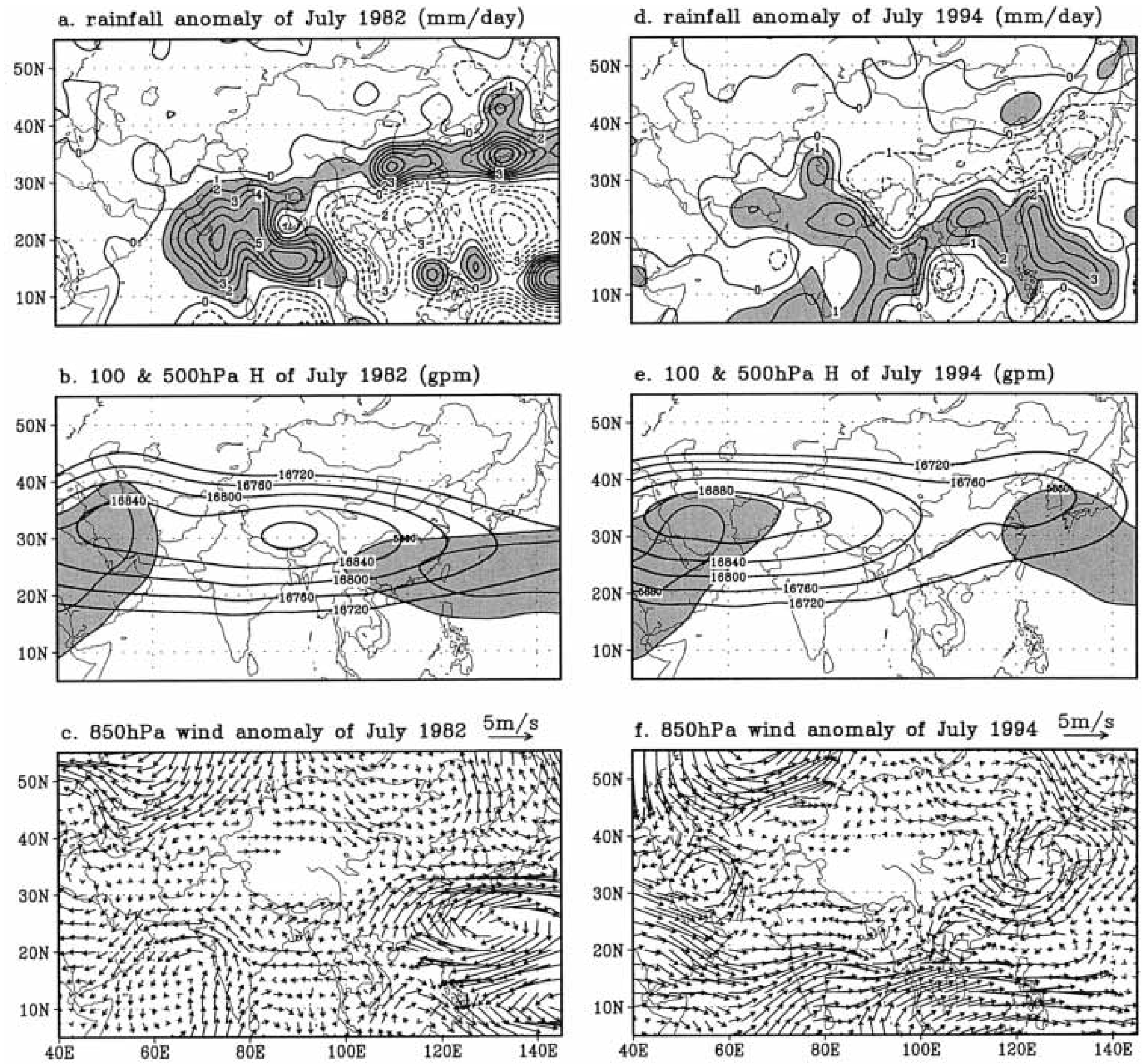

Fig. 8. Rainfall anomaly and atmospheric circulation structure for July 1982 (a, b and c) and for July 1994 (d, e and f). a and d, rainfall anomaly, those anomalies greater than 1 mm/day are shaded. b and e, 100 and 500 hPa geopotential height distribution, those greater than 5860 gpm at 500 hPa are in shading, the contour interval for 100 hPa height is 40 gpm and only those greater than 16720 gpm are plotted. c and f, 850 hPa wind anomaly, the vectors where the topography greater than 3000 m are set in default.

Acknowledgments

The authors appreciate the comments on an earlier version of the manuscript made by Dr. Tomoaki OSE and two anonymous reviewers. This study is supported by the Natural Science Foundation of China under the grant number 40005006 and 40135020, National Key Programme for Developing Basic Sciences G1998040900 and the Knowledge Innovation Key Project of Chinese Academy of Science in the Resource Environment Field under the grant number ZKCX2-203 and ZKCX2-SW-210.

References

Chen, G.Y. and Q.S. Liao, 1983: The relationship of 100 hPa South Asian High and summer precipitation in China. *Meteorological Science technique symposium*, **No. 6**, Meteorological Press, 123pp. [in Chinese]

Flohn, H., 1960: Recent investigation on the mechanism of the 'summer monsoon' of southern and eastern Asia. *Proc. Symp. Monsoon of the world*, New Delhi, Hind Union Press, 75–88.

He, H., J.W. McGinnis, Z. Song and M. Yanai, 1987: Onset of the Asian Summer Monsoon in 1979 and the effect of the Tibetan Plateau. *Mon. Wea. Rev.*, **115**, 1966–1995.

Institute of the Central Meteorological Bureau, 1978: The preliminary discussion on the east-west oscillation of the South Asian High. *Symposium paper collections on Tibetan Plateau Meteorological (1975–1976)*, Science Press, Beijing, China, 148–157. [in Chinese]

Kalnay, E. and Coauthors, 1996: The NCEP/NCAR 40-year reanalysis project. *Bull. Amer. Meteor. Soc.*, **77**, 437–471.

Krishnamurti, T.N., S.M. Daggupaty, J. Fein, M. Kanamitsu, and J.D. Lee, 1973: Tibetan High and upper tropospheric tropical circulation during Northern summer. *Bull. Amer. Meteor. Soc.*, **54**, 1234–1249.

Liu, F.M. and S.H. Wei, 1987: The east-west oscillation of the 100 hPa South Asia High and its forecasting. *The effects of the Tibetan Plateau on weather of China during summer*, Science Press, 111–117. [in Chinese]

Liu, Y.M. and G.X. Wu, 2000: Reviews on the study of the subtropical anticyclone and new insights on some fundamental problems, *Acta Meteorological Sinica*, **58**, 500–512. [in Chinese]

Luo, S.W., Z.A. Qian and Q.Q. Wang, 1982: The study for 100 mb South Asian Hiah and its association with climate of East China. *Plateau Meteorology*, **1**, 1–10. [in Chinese]

Mason, R.B. and C.E. Anderson, 1963: The development and decay of the 100 mb summertime anticyclone over Southern Asia. *Mon. Wea. Rev.*, **91**, 3–12.

Qian, Y.F., 1978: The calculation method of the heating field and the effects of the heating during a Tibetan High process, *Symposium paper collections on Tibetan Plateau Meteorological (1975–1976)*, Science Press, Beijing, China, 199–212. [in Chinese]

Tao, S.Y. and F.K. Zhu, 1964: The variation of 100 mb circulation over South Asia in summer and its association with march and withdraw of West Pacific Subtropical High. *Acta Meteorological Sinica*, **34**, 385–395. [in Chinese]

Yang, Z. and H. Yang, 1984: The relation between the South Asia High and precipitation of Qinghai Province during flood period. *Qinghai-Xizang Plateau Meteorology Experiment Symposium*, **No. 2**, Science Press, 159–171. [in Chinese]

Xie, P. and P.A. Arkin, 1997: Global precipitation: A 17-year monthly analysis based on gauge observations, satellite estimates, and numerical model outputs. *Bull. Amer. Meteor. Soc.*, **78**, 2539–2558.

Xu, B.N., 1983: Some statistical characters of the South Asia High during early summer and its relation to weather of northeast Guizhou Province. *Meteorological Science Technique Symposium*, **No. 6**, Meteorological Press, 108–115. [in Chinese]

Zhang, K.S. and D.Z. Ye, 1977: Simulation of the movements of the Tibetan High and the application on summer prediction. *Scientia Sinica*, **No. 4**, 360–368. [in Chinese]

Zhang, Q. and G.X. Wu, 2001: The large area flood and drought over Yangtze River Valley and its relation to the South Asia High. *Acta Meteorological Sinica*, **59**(5), 569–577. [in Chinese]

Zhao, W. and F.K. Zhu, 1978: Midsummer precipitation over south Xinjiang Province and the South Asia High. *Meteorology*, **No. 9.** [in Chinese]

Zhu, F.K., L.Y. Lu, X.J. Chen and W. Zhao, 1980: *The South Asia High*. Science Press, Beijing, China, 95pp. [in Chinese]